JOC The Journal of Organic Chemistry

Article

pubs.acs.org/joc

Experimental and Theoretical Insights into the Mechanisms of Sulfate and Sulfamate Ester Hydrolysis and the End Products of Type I Sulfatase Inactivation by Aryl Sulfamates

Spencer J. Williams,*[,†,‡] Emma Denehy,[†,‡] and Elizabeth H. Krenske*[,†,§,∥]

[†]School of Chemistry and [‡]Bio21 Molecular Science and Biotechnology Institute, The University of Melbourne, Melbourne, VIC 3010, Australia

[§]Australian Research Council Centre of Excellence for Free Radical Chemistry and Biotechnology

[∥]School of Chemistry and Molecular Biosciences, The University of Queensland, Brisbane, QLD 4072, Australia

Supporting Information

ABSTRACT: Type I sulfatases catalyze the hydrolysis of sulfate esters through S−O bond cleavage and possess a catalytically essential formylglycine (FGly) active-site residue that is post-translationally derived from either cysteine or serine. Type I sulfatases are inactivated by aryl sulfamates in a time-dependent, irreversible, and active-site directed manner consistent with covalent modification of the active site. We report a theoretical (SCS-MP2//B3LYP) and experimental study of the uncatalyzed and enzyme-catalyzed hydrolysis of aryl sulfates and sulfamates. In solution, aryl sulfate monoanions undergo hydrolysis by an S_N2 mechanism whereas aryl sulfamate monoanions follow an S_N1 pathway with SO_2NH as an intermediate; theory traces this difference to the markedly greater stability of SO_2NH versus SO_3. For *Pseudomonas aeruginosa* arylsulfatase-catalyzed aryl sulfate hydrolysis, Brønsted analysis ($\log(V_{max}/K_M)$ versus leaving group pK_a value) reveals $\beta_{LG} = -0.86 \pm 0.23$, consistent with an S_N2 at sulfur reaction but substantially smaller than that reported for uncatalyzed hydrolysis ($\beta_{LG} = -1.81$). Common to all proposed mechanisms of sulfatase catalysis is a sulfated FGly intermediate. Theory indicates a ≥26 kcal/mol preference for the intermediate to release HSO_4^- by an E2 mechanism, rather than alkaline phosphatase-like S_N2 substitution by water. An evaluation of the stabilities of various proposed end-products of sulfamate-induced sulfatase inactivation highlights that an imine *N*-sulfate derived from FGly is the most likely irreversible adduct.

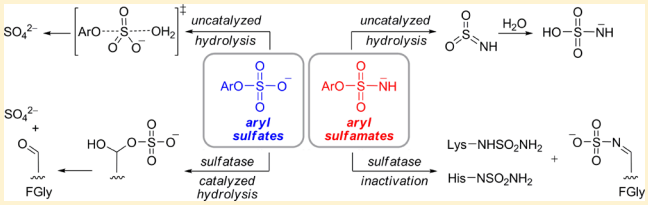

INTRODUCTION

Sulfatases are enzymes that catalyze the hydrolysis of sulfate esters (Scheme 1a) in a diverse range of sulfated substrates including steroids, hormones, and various glycoconjugates including glucosinolates, glycosaminoglycans, proteoglycans, and glycolipids. Type I sulfatases[1] require a post-translational modification of a cysteine or serine residue to a catalytically essential formylglycine (FGly) residue.[2] The FGly-dependent, type I sulfatases have emerged as important targets for drug development, owing to their roles in hormone regulation, developmental cell signaling, bone development, and bacterial pathogenesis.[3] One of the most potent classes of inhibitors of type I sulfatases are aryl sulfamates $(ArO)SO_2NH_2$.[4,5] Aryl sulfamates have been developed as inhibitors of the enzyme steroid sulfatase (Scheme 1b), and 667COUMATE (STX64, Irosustat) and PGL2001 have entered clinical trials against hormone-dependent breast, endometrial, and prostate cancers and endometriosis, respectively.[6]

Type I sulfatases display a highly conserved three-dimensional fold, active-site residues, and active-site geometry, consistent with a conserved catalytic mechanism.[3,7] The active site contains the FGly residue, several positively charged amino acids (Lys and His), and a divalent metal cation (Ca^{2+} or Mg^{2+}). Two different catalytic mechanisms have been proposed, featuring different roles for the FGly residue (Scheme 2). Guss et al.[8] proposed that the FGly aldehyde undergoes nucleophilic attack by the sulfate ester anion (Scheme 2a) giving diester **A**. Hydrolysis of **A** liberates ROH and gives the intermediate **B**, which eliminates HSO_4^- to regenerate the FGly aldehyde. In an alternative mechanism, proposed by von Figura and Saenger et al.[9] (Scheme 2b), the active form of FGly is the hydrate **C**, which performs a nucleophilic substitution on the sulfate ester anion to give **B** directly. Elimination and rehydration complete the catalytic cycle. X-ray crystal structures of human sulfatases provide evidence for the existence of both **B** and **C** but do not necessarily demonstrate that these species lie on the reaction coordinate.[8,9] One indirect piece of evidence supporting pathway (b) is the finding that when the Cys→FGly post-translational modification is blocked (Scheme 2, box (i)) by a Cys→Ser mutation the mutant enzyme processes the substrate as far as **B′** but cannot release HSO_4^- to complete turnover under acidic conditions.[10−12] However, it is not clear whether

Received: December 1, 2013
Published: February 20, 2014

   dx.doi.org/10.1021/jo4026513 | J. Org. Chem. 2014, 79, 1995−2005

Scheme 1. (a) Hydrolysis of Sulfate Esters; (b) Aryl Sulfamate Inhibitors of Sulfatases

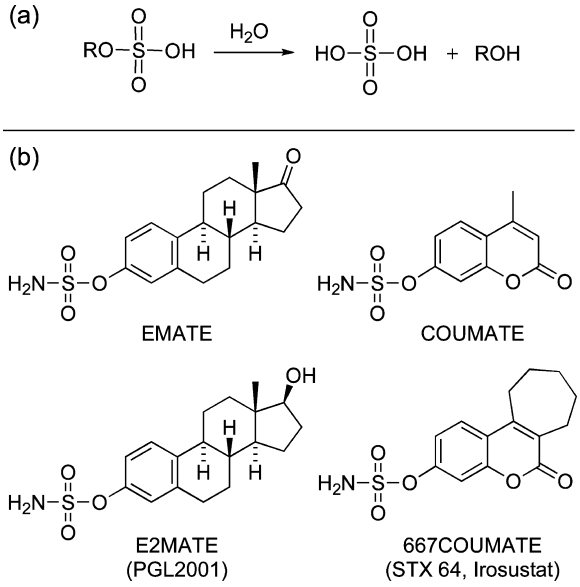

the rate of formation of the Ser-sulfate species is comparable to that for the formation of the FGly-sulfate intermediate, and thus, the relevance of this species, and indeed of all crystallographically observed species, to bonafide species along the reaction coordinate of the enzyme-catalyzed reaction is uncertain. Indeed, under basic conditions, the sulfate group of **B**′ formed on the C69S mutant of human arylsulfatase A[10] or the C51S mutant of *Pseudomonas aeruginosa* *Pa*AtsA[14b] is cleaved; in the case of human arylsulfatase B the equivalent species is stable to high pH.[10]

While mutagenesis data provide strong evidence for the requirement of an FGly residue for type I sulfatase catalysis, the reason why FGly is essential for catalytic turnover has not yet been explained. The loss of catalytic function in the absence of the FGly post-translational modification is noteworthy when considered in light of the related enzyme, alkaline phosphatase. The latter shares a high degree of structural similarity with type I sulfatases, including key residues in the active site,[8,9] but utilizes serine rather than FGly as a catalytic nucleophile to mediate the hydrolysis of phosphate monoesters (Scheme 2, box (ii)).[13] In this case, HPO_4^{2-} is efficiently released from the phosphoserine intermediate **B**″ upon attack by a metal-bound hydroxide. Conversely, the arylsulfatase *Pa*AtsA shows a rate acceleration of 10^{13} for phosphate ester hydrolysis (compared to 10^{18} for sulfate hydrolysis), demonstrating that the type I sulfatases can promiscuously catalyze phosphate ester hydrolysis, ostensibly through an equivalent FGly-dependent catalytic mechanism.[14] Interestingly, an FGly-dependent phosphonate monoester hydrolase/phosphodiesterase has been discovered that appears to catalyze hydrolysis through an identical mechanism to sulfatases.[15] While this enzyme exhibits burst kinetics, this is consistent with a two-step hydrolysis mechanism that proceeds through an intermediate, and thus this data alone does not allow the definitive assignment of either mechanisms of type (a) or type (b) (Scheme 2).

The mechanism of irreversible inhibition of sulfatases by aryl sulfamates is also not understood. Inactivation is time-dependent, active site-directed, and irreversible, consistent with a covalent chemical modification of an active site residue or residues. Using Brønsted analysis, we recently reported that the irreversible inactivation of *Pa*AtsA by aryl sulfamates involves cleavage of the ArO–S bond, and studies of stoichiometry revealed that inactivation consumes three to six molecules of sulfamate per molecule of enzyme (depending on the structure of the inhibitor).[5] Despite efforts to identify the inactivated enzyme by electrospray-ionization mass spectrometry, no evidence could be found as to the nature of the proposed covalent modification. Elucidating the nature of the covalent modification(s) remains an important goal not only for the sake of understanding the fundamental mechanism of inhibition but also for its implications regarding the potential immunogenicity of sulfamates as drug candidates.

In this paper, we seek to clarify several aspects of the mechanisms of sulfatase catalysis and inactivation. We begin with a quantum mechanical study of the uncatalyzed hydrolysis of aryl sulfates and sulfamates in alkaline solution (conditions relevant to reactions mediated by the enzyme). The anions of aryl sulfates and sulfamates are known to undergo hydrolysis by different mechanisms, S_N2 for sulfates and S_N1 for sulfamates, and we perform calculations to understand the origins of this difference. We next report a Brønsted analysis for type I sulfatase hydrolysis of aryl sulfates that provides evidence for an S_N2 reaction at sulfur, consistent with the formation of an FGly–sulfate adduct, and provides insight into the differences in catalyzed and uncatalyzed solvolysis reactions. We use theory to examine the product release step of sulfatase catalysis in order to understand the importance of the FGly post-translational modification, that is, the quantitative effect of the geminal OH group in the conversion of **B** to FGly + HSO_4^- (Scheme 2). Finally, we evaluate a series of structures that have been proposed for the dead-end products of aryl sulfamate-induced inactivation of sulfatases. Our results predict that sulfamoylation of active-site nucleophiles is an equilibrium process dependent on the nature of the leaving group on the sulfamate. A promising candidate for an irreversible covalent modification is revealed to be the imine *N*-sulfate derived from FGly.

RESULTS AND DISCUSSION

1. Mechanisms of Uncatalyzed Hydrolysis of Aryl Sulfate and Sulfamate Anions. The active sites of type I sulfatases contain numerous anion-binding groups including an array of basic residues (arginine, lysine, histidine) and a divalent metal ion (Mg^{2+} or Ca^{2+}). Thus, the ionization state of sulfate and sulfamate esters relevant to sulfatase activity or inhibition is the monoanion $(RO)SO_2X^-$ (X = O, NH). The mechanisms of uncatalyzed hydrolysis of aryl sulfate and sulfamate monoanions in aqueous and organic media have been studied extensively,[16−26] and the parallels and divergences between the mechanisms of sulfate hydrolysis and phosphate ester hydrolysis have been described in the literature.[13] The alkaline hydrolysis of an aryl sulfate (anion) has a negative activation entropy (−19 eu for *p*-nitrophenyl sulfate at 35 °C),[16,18] and variation of the leaving group produces a Brønsted plot (log *k* against the pK_a value of the corresponding phenol) for hydrolysis at 25 °C having a slope of $\beta_{LG} = -1.81$.[27,28] These features have been interpreted as indicating a concerted reaction, with a loose transition state in which S–O bond cleavage is much more advanced than bond formation to the nucleophile (H_2O).[13,18] The reaction is formally an $S_N2@S$ process.[19] For aryl sulfamate anions (X = NH or NMe), hydrolysis follows a different mechanism. Describing the

dx.doi.org/10.1021/jo4026513 | J. Org. Chem. 2014, 79, 1995−2005

Scheme 2. (a,b) Two Proposed Mechanisms for Sulfate Ester Hydrolysis by Type I Sulfatases[a,8,9]

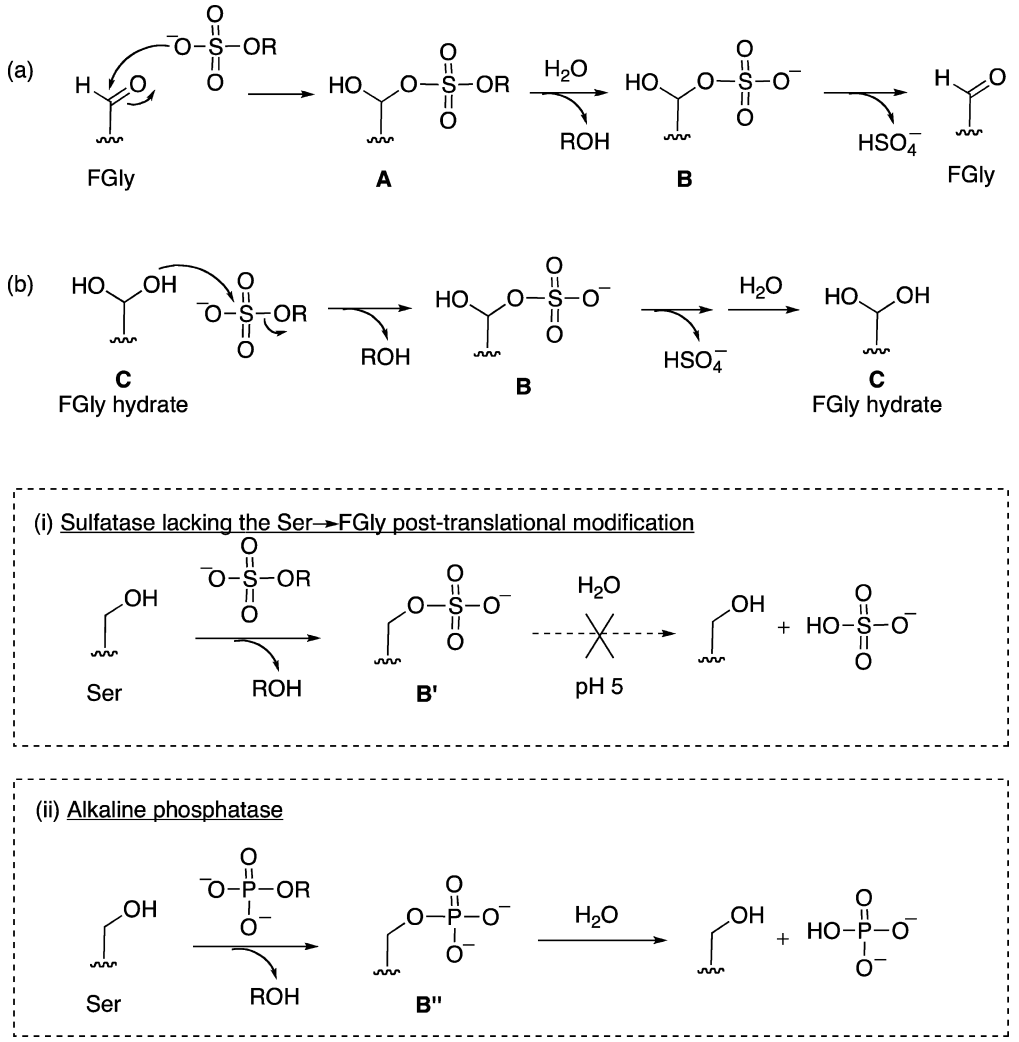

[a]Inset i shows the arrested turnover in the absence of the FGly post-translational modification in a Cys→Ser mutant.[10] Inset ii shows the mechanism of phosphate ester hydrolysis by alkaline phosphatase, involving a catalytic serine residue.[13]

reaction with reference to the neutral reactant, the initial phase is an E1cb elimination that generates the sulfonylamine SO_2NH or SO_2NMe.[21−24] This intermediate reacts with the nucleophile. In our discussion of mechanisms below, we will use a terminology where the reference species is the sulfamate monoanion, in which case the hydrolysis is classified overall as an S_N1@S process. The leaving-group Brønsted coefficients for alkaline hydrolysis of aryl sulfamates are $\beta_{LG} = -1.2$ (X = NH)[21] and −1.8 (X = NMe).[24]

Calculations were performed to understand why aryl sulfate and sulfamate monoanions follow different hydrolysis mechanisms. The mechanisms of related phosphate ester hydrolysis reactions have been the subject of a number of sophisticated mixed quantum mechanical/molecular mechanical simulations (QM/MM).[29] We have employed here a purely QM approach (SCS-MP2/6-311+G(d,p)//CPCM/B3LYP/6-31+G(d)) to examine the features of sulfate and sulfamate ester hydrolysis. This approach is informed by a recent study by Kamerlin, who utilized COSMO/B3LYP/6-311+G(d,p)//PCM/B3LYP/6-31+G(d) calculations to map out in detail the potential energy surfaces for hydrolysis of *p*-nitrophenyl sulfate and phosphate esters in solution.[30]

In aqueous solution at physiologically relevant pH, the likely nucleophile is a water molecule.[16−18] In our calculations, difficulties in locating transition states involving water as the nucleophile prompted the study of OH^- as a model nucleophile. The resulting energy profiles do not allow a quantitative prediction of rates but instead serve our purpose of comparing how the two hydrolytic pathways differ for sulfamates versus sulfates. The two alternative pathways for sulfate and sulfamate hydrolysis are shown diverging from the central box at the top of Figure 1. The lower panel of Figure 1 shows the calculated free energy profiles for hydrolysis of *p*-nitrophenyl sulfate (**1**) and sulfamate (**2**) monoanions in water occurring by the S_N2 (path A) or S_N1 (path B) mechanisms. In the S_N1 pathway, the cleavage of the ArO−S bond (and formation of the HO−S bond of the product) was found to be a barrierless process on the potential energy surface.[31] The intermediates **IntB** (*p*-nitrophenolate + SO_2X) therefore represent the maxima along the S_N1 reaction coordinates.

The S_N2 transition states with OH^- are expected to be higher in energy than those with water because of charge repulsion between the electrophile and the nucleophile and because the large solvation energy of OH^- will raise the solution-phase

dx.doi.org/10.1021/jo4026513 | J. Org. Chem. 2014, 79, 1995−2005

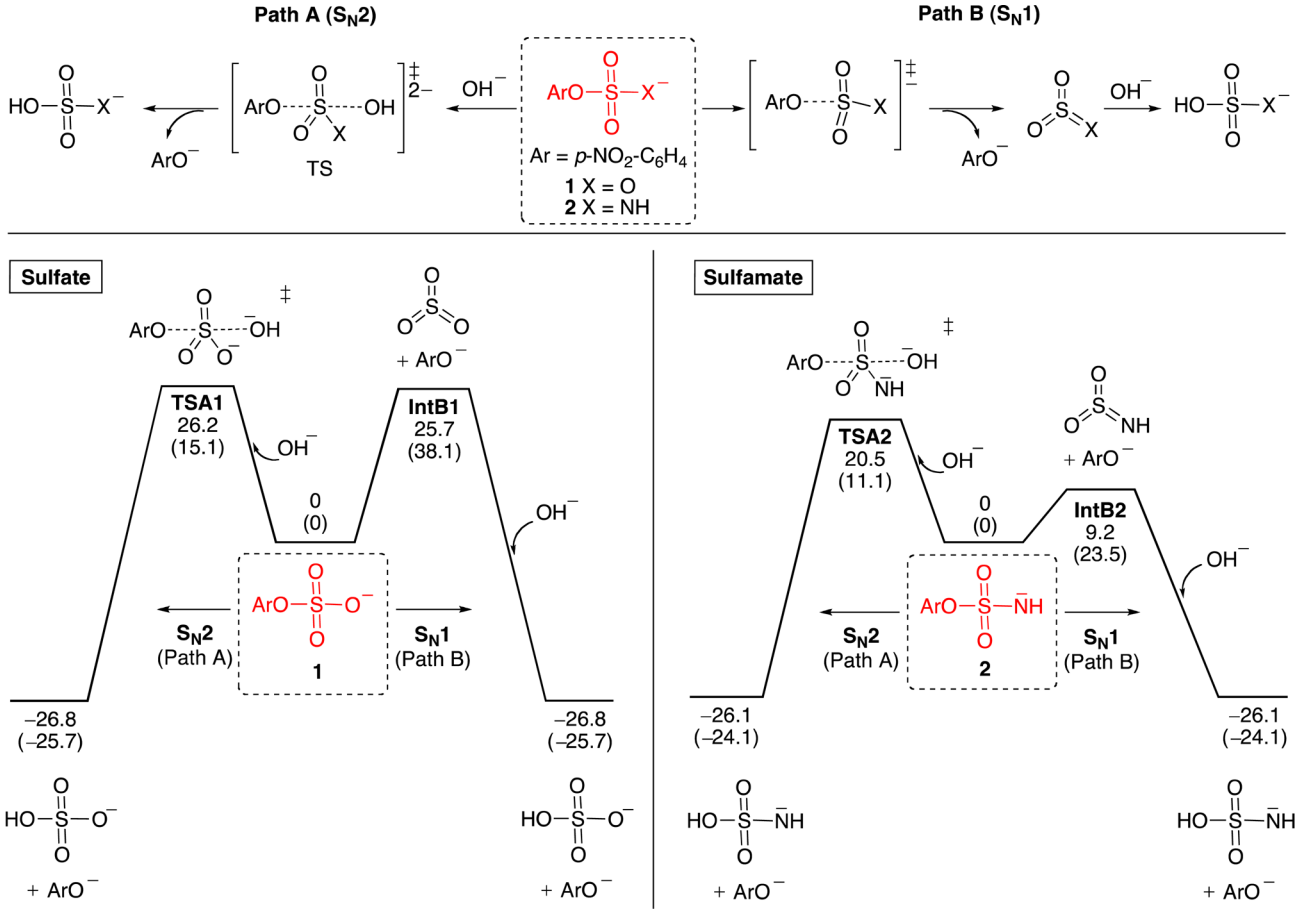

Figure 1. Free energy profiles for hydrolysis of *p*-nitrophenyl sulfate and sulfamate monoanions proceeding through S_N2 or S_N1 mechanisms. Free energies in water (with enthalpies in parentheses) were computed at the SCS-MP2/6-311+G(d,p)//CPCM/B3LYP/6-31+G(d) level of theory.

barrier. This explains why the energy profiles in Figure 1 appear incorrectly to slightly favor an S_N1 pathway for **1** even though the experimental data[13,16−19] point to an S_N2 mechanism (H_2O as nucleophile). However, meaningful insights can be derived from the way that the energy of a given pathway changes upon going from **1** to **2**. Such comparisons do correctly capture the trends observed experimentally.[32] That is, when comparing **1** with **2** the S_N1 pathway drops by 16.5 kcal/mol, consistent with the known switch to the S_N1 hydrolysis mechanism on going from **1** to **2**. Interestingly, the S_N2 transition state also drops (by 5.7 kcal/mol) on going from **1** to **2**, but this is overshadowed by the very large acceleration of the S_N1 pathway, which accounts for the difference in mechanism for the two substrates. These features of the reaction profiles are mirrored by calculations performed at a range of other levels of theory (see the Supporting Information).

We examined how the S_N1 and S_N2 barriers are influenced by the leaving group. For **1**, replacement of the *p*-nitrophenolate leaving group by the poorer leaving group phenolate in **3** raised the S_N2 barrier by 6.3 kcal/mol and the S_N1 barrier by 10.7 kcal/mol. For **2**, the change to a phenolate leaving group in **4** raised the S_N2 barrier by 8.2 kcal/mol and the S_N1 barrier by 11.4 kcal/mol. These values suggest that the S_N1 barrier is more susceptible to leaving group effects and that the *p*-NO_2 substituent contributes about 3 kcal/mol toward the S_N1 preference of sulfamate **2**.

Why does the preferred pathway switch from S_N2 to S_N1 on going from aryl sulfate to aryl sulfamate? The isodesmic reactions in eqs 1 and 2 were computed to determine whether the small S_N1 barrier for a sulfamate anion results from

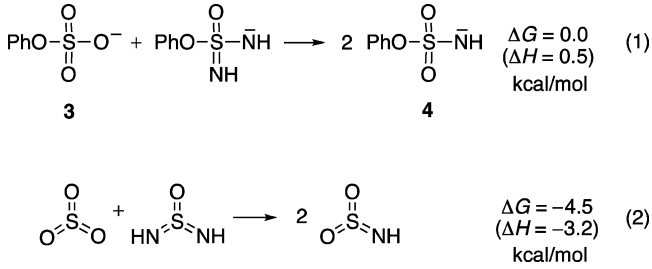

stabilization of the intermediate SO_2NH or from destabilization of the reactant. Equation 1 indicates that replacement of one of the S═O groups in $(PhO)SO_3^-$ by S═NH (**3** → **4**) has only a marginal effect on stability. In contrast, replacement of one of the S═O groups in SO_3 by S═NH (eq 2) leads to 4.5 kcal/mol of stabilization. Therefore, the ease of S_N1 hydrolysis of **2** is traced to the enhanced stability of the intermediate SO_2NH.

The S═O → S═NH substitution dramatically lowers the barrier for S_N1 dissociation (Figure 1). To explore how this reaction may be influenced by different NR substituents, we computed the dissociation energies of a range of other sulfamates (**4**–**9**, Table 1). The nitrogen substituent effects are found to span a range of 26 kcal/mol; the most readily dissociable substrate is the NMe derivative **5** (ΔG = 16.1 kcal/mol) and the least readily dissociable is the NCN derivative **9** (ΔG = 42.2 kcal/mol). Dissociation becomes more favorable as

dx.doi.org/10.1021/jo4026513 | J. Org. Chem. 2014, 79, 1995−2005

Table 1. Calculated Energies of S_N1 Dissociation of Phenyl Sulfate, Sulfamate, and Sulfonate Anions[a]

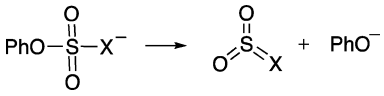

X	ΔG (ΔH)
O (**3**)	36.4 (49.3)
NH (**4**)	20.6 (34.1)
NMe (**5**)	16.1 (31.5)
NPh (**6**)	24.2 (38.9)
NC_6H_4OMe (**7**)	22.8 (37.4)
$NC_6H_4NO_2$ (**8**)	27.0 (42.1)
N(CN) (**9**)	42.2 (56.1)
CH_2 (**10**)	5.7 (19.3)

[a]SCS-MP2/6-311+G(d,p)//CPCM(water)/B3LYP/6-31+G(d), kcal/mol.

the electron-donor capacity of R increases. In the N(Ar) series (**6**–**8**), a MeO group at the *para* position yields a 4.2 kcal/mol lower dissociation energy than a *p*-NO_2 group. The increased propensity toward dissociation when nitrogen bears an electron-donating group reflects the fact that the donor enables the resonance scheme for SO_2X (Scheme 3) to secure greater benefit from contributions such as **11d**.

Scheme 3. Resonance Structures of SO_2X

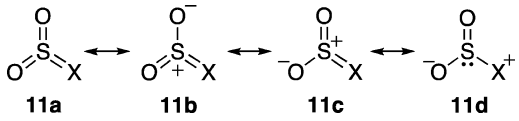

Extending the trend observed on going from X = O to X = NR, the sulfonate **10** (X = CH_2) is computed to dissociate to phenoxide plus sulfene (SO_2CH_2) with an energy of only 5.7 kcal/mol (Table 1). Experimentally, SO_2CH_2 has been generated from methanesulfonyl chloride by treatment with base.[33] The reaction of *p*-nitrophenyl methanesulfonate with OH^- is believed to occur by an addition–elimination mechanism, rather than through the intermediacy of sulfene, presumably because the high pK_a value of the ester prevents the deprotonation step of the E1cb pathway in aqueous solution.[34] Stabilized sulfenes (e.g., SO_2CHAr) have, however, been identified as intermediates in the alkaline hydrolysis of aryl phenylmethanesulfonates.[34]

2. Mechanism of Sulfatase-Catalyzed Hydrolysis of Aryl Sulfates. While there are several reports of linear free energy analysis of sulfatase catalysis,[35] this data dates from before the genomic era and prior to the recognition of the need for the FGly mutation for type I sulfatase activity, and thus, the relationship of these enzymes and the accompanying data to the mechanisms of type I sulfatases cannot be ascertained. *Pa*AtsA is a widely used model for type I sulfatases as it can be readily expressed in recombinant form with the FGly modification in *E. coli*[36] and has activity on a range of substituted aryl sulfates. A range of aryl sulfates with varying leaving group pK_a values were synthesized,[25a] and Michaelis–Menten parameters were measured (Table 2). The values in Table 2 reveal little variation in V_{max}, suggesting that the leaving group is not involved in the rate-determining step. On the other hand, a clear trend is evident in V_{max}/K_M, which reflects the first irreversible chemical step. While the Brønsted plot of log(V_{max}/K_M) versus leaving group pK_a values displays significant scatter, the data can be fitted to a simple linear regression model that reveals a steep dependence (β_{LG} = −0.86 ± 0.23) of the second-order rate constant (Figure 2). The

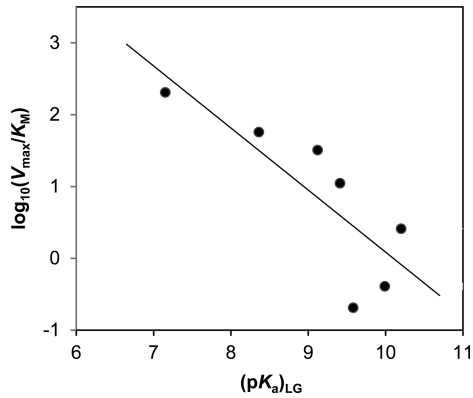

Figure 2. Brønsted plot of *Pa*AtsA-catalyzed hydrolysis of aryl sulfate monoesters.

relatively large magnitude of the slope indicates a large degree of charge development associated with bond cleavage to the leaving group at the transition state and suggests little general acid catalysis. This data does not alone provide unambiguous evidence to distinguish between mechanisms (a) or (b); in particular, if the first step of mechanism (a) (FGly→**A**) is reversible, then this data equally supports both mechanisms. Nonetheless, this data provides strong evidence for an S_N2@S process. It is interesting to compare the slope of the Brønsted plot for the enzyme-catalyzed reaction for *Pa*AtsA with that measured for the hydrolysis of a series of arylsulfates (log *k* against leaving group pK_a value) which displayed a very steep slope with β_{LG} = −1.81.[27,28] As both of these reactions are S_N2@S processes, the origin of the difference in the β_{LG} values may arise from the absence or presence of general base catalysis assisting nucleophile attack, synchronized transition-state stabilization by the enzyme versus incomplete rearrangement

Table 2. Michaelis–Menten Parameters for the Hydrolysis of Arylsulfate Monoesters by *Pa*AtsA

substrate	pK_a	K_M (mM)	V_{max} (mM mg^{-1} s^{-1}) × 10^{-1}	V_{max}/K_M (mg^{-1} s^{-1})
4-NO_2	7.15	(1.75 ± 0.02) × 10^{-3}	3.58 ± 0.04	(2.04 ± 0.05) × 10^2
3-NO_2	8.36	(1.54 ± 0.10) × 10^{-2}	8.82 ± 0.21	(5.72 ± 0.51) × 10^1
3-Cl	9.12	(2.48 ± 0.17) × 10^{-2}	7.97 ± 0.15	(3.21 ± 0.28) × 10^1
4-Cl	9.41	(6.66 ± 0.15) × 10^{-2}	7.36 ± 0.04	(1.11 ± 0.04) × 10^1
4-NHAc	9.58	1.68 ± 0.11	3.43 ± 0.07	(2.05 ± 0.18) × 10^{-1}
H	9.99	1.63 ± 0.08	6.65 ± 0.17	(4.07 ± 0.30) × 10^{-1}
4-MeO	10.20	(3.66 ± 0.12) × 10^{-1}	9.44 ± 0.11	2.58 ± 0.11

dx.doi.org/10.1021/jo4026513 | J. Org. Chem. 2014, 79, 1995–2005

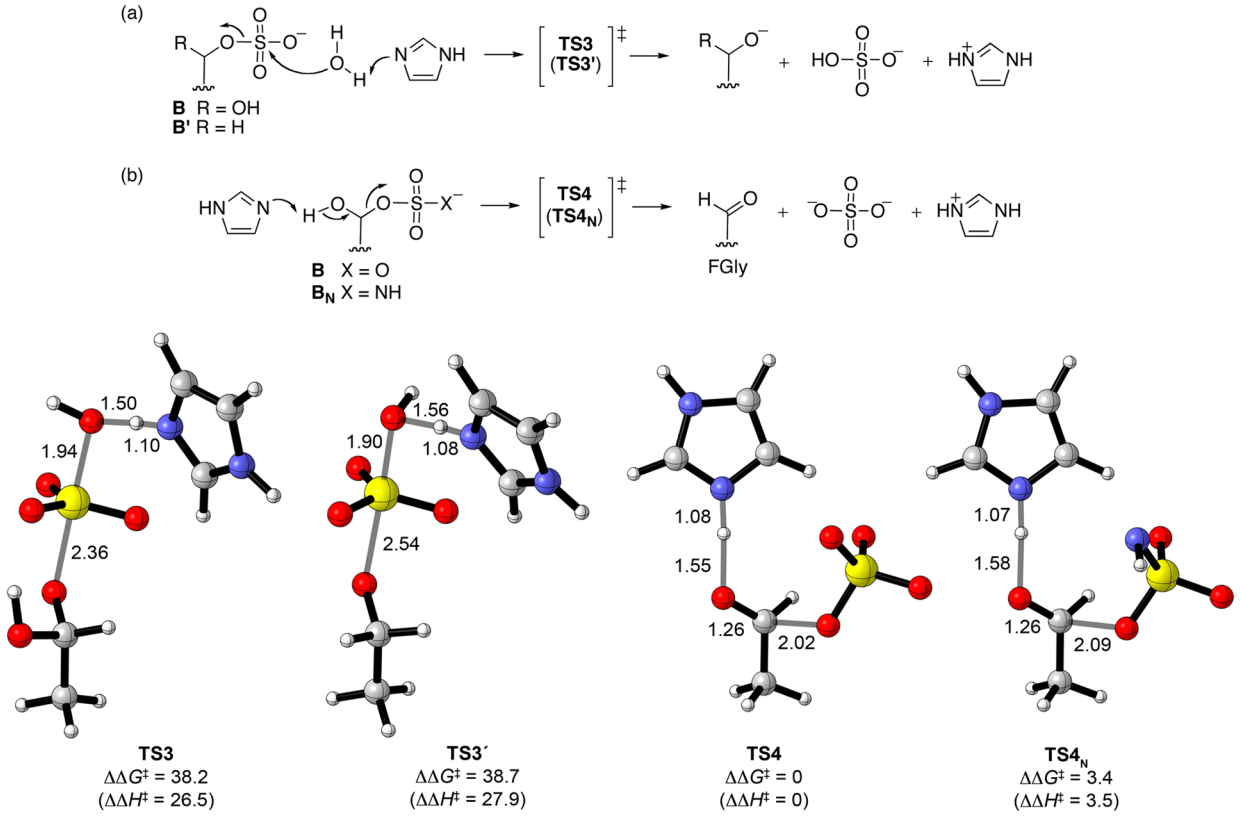

Figure 3. Transition states for release of HSO_4^- (or HSO_3NH^-) from enzyme-bound intermediates according to (a) S_N2 or (b) E2 mechanisms. Values of $\Delta\Delta G^‡$ and $\Delta\Delta H^‡$ indicate that the E2 mechanism of product release is strongly favored over the S_N2 mechanism.

of solvation in solution, and differing degrees of (weak) general acid assistance (or metal ion coordination) facilitating leaving group departure. Importantly, the available crystallographic data for type I sulfatases indicate the presence of likely amino acid candidates able to play the role of general base and general acid, as well as metal ions that may fulfill these roles.[8,9,36] According to this interpretation, the β_{LG} data suggest that the uncatalyzed hydrolysis transition state is loose, with extensive bond fission to the leaving group, whereas the enzyme-catalyzed transition state is tighter and less dissociative in character. Alternatively, the lower slope may be a result of charge neutralization at the leaving group oxygen by partial protonation (or metal ion coordination) at the transition state.

Experiments on a sulfatase mutant possessing a Ser in place of the FGly post-translational modification (Scheme 2, box (i)) indicated that the serine mutant was capable of displacing aryloxide from *p*-nitrocatechol sulfate, to generate intermediate **B**′, but the mutant could not complete a catalytic cycle by releasing HSO_4^- at pH 5.[10] As **B** features in both mechanisms (a) and (b) this suggests that the geminal OH group of the FGly-derived intermediate **B** is essential for HSO_4^- cleavage. It has been proposed[10,36] that HSO_4^- release involves cleavage of the C−O bond, induced by deprotonation of the geminal OH (Figure 3b). Therefore, to evaluate the quantitative effect of the geminal OH group (i.e., **B** vs **B**′), we compared the elimination with an alternative mechanism of HSO_4^- release involving S_N2 displacement at sulfur by water (Figure 3a). Both mechanisms involve general base catalysis, and we used imidazole to model the histidine residue that is proposed to function as a general base in the enzyme-catalyzed reaction.[3,36]

The calculated transition states for the two product release pathways are shown in Figure 3 (**TS3**, **TS4**). Also shown is the corresponding transition state for an S_N2-like substitution mechanism in the FGly→Ser mutant (**TS3**′). The relative activation energies ($\Delta\Delta G^‡$ and $\Delta\Delta H^‡$) enable a direct comparison of the likelihood of the different pathways.[37] Comparison of **TS3** with **TS3**′ indicates that the geminal OH group has only a small effect on the activation energy for the S_N2 substitution ($\Delta\Delta G^‡$ = 0.5 kcal/mol), hardly enough to account for the arrested turnover of the serine mutant. Instead, the calculations show that release of HSO_4^- by the E2 route (**TS4**) is enormously favored. The difference in $\Delta\Delta H^‡$ between **TS4** and **TS3** is 26.5 kcal/mol. The difference in $\Delta\Delta G^‡$ is 12 kcal/mol greater than this, reflecting the fact that **TS3** is formally trimolecular while **TS4** is bimolecular. While the absolute magnitudes of $\Delta G^‡$ and $\Delta H^‡$ cannot be compared with those of the other steps in the catalytic mechanism (since they do not attempt to take account of the stabilizing roles of active-site groups), the models do give an indication of the underlying feasibilities of the two product release mechanisms under the minimal conditions for catalysis. The markedly lower barrier for **TS4** (cf. **TS3**) supports the view that the E2 process is the most likely mechanism of HSO_4^- release from sulfated FGly, as has been suggested previously,[3,10] and indicates why the serine mutant is incapable of catalytic turnover. A recent study[38] of the mechanism of *Pa*AtsA-catalyzed hydrolysis of *p*-nitrophenyl sulfate assumed that the sulfate release step follows an E2 mechanism; in this study, several active-site residues and a Ca^{2+} ion were treated by a QM cluster approach, and the E2 transition state liberating SO_4^{2-} was found to lie only 2.6 kcal/mol higher than the preceding intermediate.

These results inspire the question: why has nature chosen FGly for the catalytic nucleophile in type I sulfatases but serine in alkaline phosphatase? That is, does sulfate release pose some

dx.doi.org/10.1021/jo4026513 | J. Org. Chem. 2014, 79, 1995−2005

inherent difficulty compared to the hydrolysis of a phosphoserine intermediate? To explore this, we calculated transition states analogous to **TS3** and **TS4** for a FGly–phosphate adduct bearing the same overall charge as FGly–sulfate adduct **B** (Scheme 4). Aside from the promiscuous phosphatase activity

Scheme 4. S_N2 and E2 Pathways for Phosphate Release from a Hypothetical FGly–Phosphate Adduct

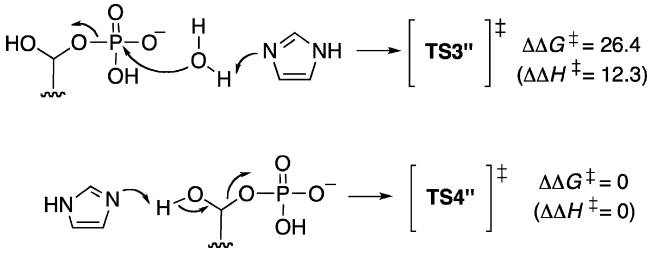

observed for *Pa*AtsA, evidence for the existence of an FGly–phosphate species has been obtained in the X-ray crystal structure of human arylsulfatase A, which after incubation with a phosphate monoester showed a covalently bound phosphate attached to the active site FGly.[39] Our calculations reveal that although the E2 pathway of phosphate release (**TS4″**) is favored over the S_N2 pathway (**TS3″**), the difference between the two release mechanisms is much smaller than in the sulfate case. The E2 TS for phosphate release is preferred by just 12.3 kcal/mol ($\Delta\Delta H^{\ddagger}$), compared to 26.5 kcal/mol for sulfate release. In their QM cluster model study[38,40] of the promiscuous phosphatase activity of *Pa*AtsA, Marino et al. found that when the phosphate bears an additional negative charge the E2 elimination recruits general acid assistance from an active-site carboxylic acid relayed through a water molecule, which is not required for the sulfate reaction. It has been suggested that the E2 product release pathway involving the FGly geminal OH group may be evolutionarily tied to the need for sulfatases to be active in acidic environments.[10] Our calculations confirm that sulfate is a much poorer leaving group in the S_N2 release pathway, which perhaps provided the impetus for the evolution of the alternative E2 pathway as proposed by Hyvönen and Hollfelder.[41] Indeed, Edwards and Wolfenden reported Brønsted analysis comparing the hydrolytic rates of sulfate and phosphate monoesters.[27] The gradient of the plot for the reaction of sulfate monoesters was significantly steeper ($\beta_{LG} = -1.75$) than that for the phosphate monoester dianions ($\beta_{LG} = -1.26$), resulting in a divergence of reactivity such that while 2,4-dinitrophenyl phosphate and sulfate possessed similar reactivity, the rate of pentyl phosphate hydrolysis was estimated to be 10^5-fold faster than pentyl sulfate.

3. Mechanisms of Covalent Modification of Sulfatases by Aryl Sulfamates. Aryl sulfamates are potent irreversible inactivators of type I sulfatases, but the nature of the covalent modification(s) leading to irreversible inactivation remains poorly understood. A Brønsted plot of *Pa*AtsA inactivation by aryl sulfamates (k_{inact}/K_I) possessed a steep slope ($\beta_{LG} = -1.1$), suggesting that the transition state for the first irreversible chemical step of inactivation involves a high degree of charge transfer and cleavage of the ArO–S bond.[5a] Accordingly, a range of sulfamoylated structures have been proposed (Scheme 5).[4c–e,5a,42] Sulfamoylation of active-site lysine (**12**) and histidine (**13**) residues is conceivable (as well as FGly **14**) if the sulfamate dissociates in the active site and SO_2NH is

Scheme 5. Proposed Structures for the End Product of Inactivation of Sulfatases by Aryl Sulfamates[4c–e,5a,42]

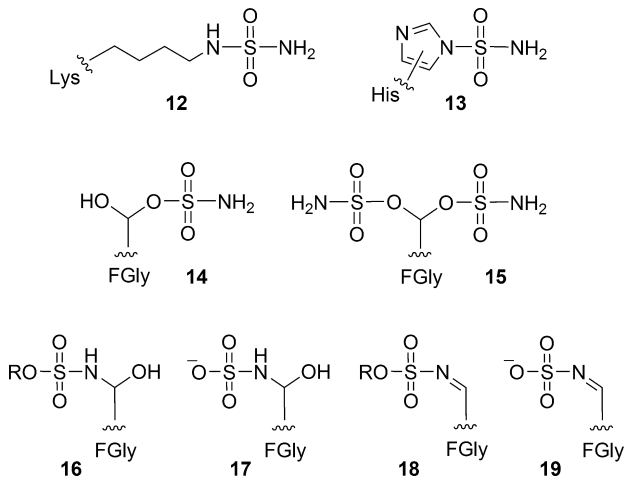

trapped by one of these residues. The doubly sulfamoylated FGly residue **15** represents another possible dead-end product, which cannot release SO_2NH by an E2 pathway. The imine *N*-sulfate **19** has been proposed[4d] to result from addition of the sulfamate amino group to FGly aldehyde, possibly involving **16** and either **17** or **18** as an intermediate; alternatively it could be formed by reaction of FGly aldehyde with HSO_3NH^-.[4e] To evaluate the stabilities of these proposed dead-end products, we computed the energies of transfer of SO_2NH from (PhO)-SO_2NH^- (**4**) to model active-site residues, as shown in Table 3.

The transfer of a sulfamoyl group from phenyl sulfamate anion to FGly is computed to be almost thermoneutral (ΔH = −2.8 kcal/mol, ΔG = −0.9 kcal/mol). A transition state for the elimination of SO_2NH from the resulting adduct **20** by an E2 mechanism (the same mechanism predicted for sulfate release) was computed and is shown in Figure 3 (**$TS4_N$**). The calculated activation energy is 3.4 kcal/mol higher than that for sulfate release. This may be sufficient to make **20** substantially longer lived than the corresponding sulfoenzyme intermediate **B**. Transfer of a sulfamoyl group from phenyl sulfamate anion to Lys or His is comparable in energy to the transfer to FGly (ΔH = −2.1 to 0.6 kcal/mol, ΔG = −1.7 to 1.5 kcal/mol). The small values of ΔG for sulfamoylation of FGly, Lys, and His suggest that these covalent modifications are likely to be reversible and, indeed, may be intercepted by water leading to nondeactivating hydrolysis of the arylsulfamate, thereby explaining the >1 stoichiometry of sulfamate inactivation. The position of the equilibrium for sulfamoyl group transfer between the aryl sulfamate and the enzyme will also be influenced by the acid–base equilibria of the released phenol. While the calculations in Table 3 pertain to phenoxide as a leaving group, experimental studies indicate that electron-withdrawing substituents increase the potency of aryl sulfamates as sulfatase inhibitors.[5] Double sulfamoylation of FGly (adduct **21**) appears not to be favorable, having ΔG = 18.3 kcal/mol. On the other hand, the imine *N*-sulfate **24** is predicted to be a very stable adduct. Formation of **24** from FGly and phenyl sulfamate anion has a free energy of −29.6 kcal/mol. This reaction, if it indeed occurs, would be much less reversible than the sulfamoylation of nucleophilic active site residues. While the effect of Lys and His sulfamoylation on sulfatase activity cannot be predicted, the irreversible conversion of the catalytically essential FGly residue

dx.doi.org/10.1021/jo4026513 | J. Org. Chem. 2014, 79, 1995–2005

Table 3. Energies of Sulfamoylation of Model Sulfatase Active Site Residues by $(PhO)SO_2NH^-$[a]

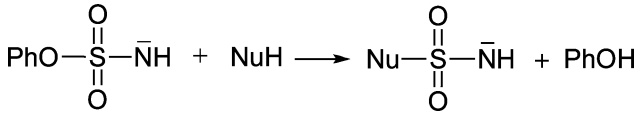

Enzyme nucleophile	NuH	Adduct	ΔG (ΔH)
FGly	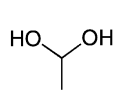	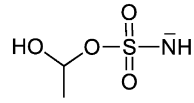 **20**	-0.9 (-2.8)
Sulfamoylated FGly	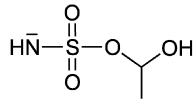	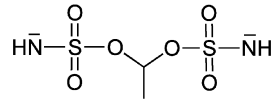 **21**	18.3 (17.9)
Lys	$Me-NH_2$	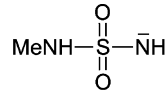 **22**	1.5 (0.6)
His		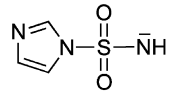 **23**	-1.7 (-2.1)
FGly (via aldehyde form)	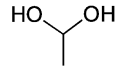	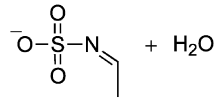 **24**	-29.6 (-17.6)

[a]SCS-MP2/6-311+G(d,p)//CPCM(Et_2O)/B3LYP/6-31+G(d), kcal/mol.

Scheme 6. Potter's Proposed Mechanism for Formation of an Azomethine Adduct of *o*-Nitrophenol 27 as a Minor Product during Synthesis of Sulfamate 26[4c]

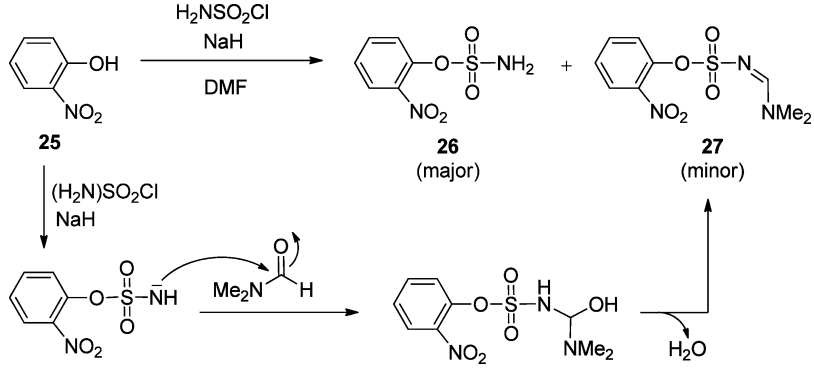

to an imine *N*-sulfate is almost certain to eliminate catalytic activity.

How might the imine *N*-sulfate form? Three possibilities appear likely. In related work, Potter reported[4c] that azomethine adduct **27** was obtained as a minor product during the base-catalyzed sulfamoylation of *o*-nitrophenol (**25**) with sulfamoyl chloride in DMF (Scheme 6). Potter suggested a mechanism involving nucleophilic addition of the sulfamate anion to the carbonyl group of DMF. A similar mechanism may be involved in imine *N*-sulfate formation from FGly, although in this case the OAr group would need to be cleaved either before or after dehydration takes place. Two alternative mechanisms are shown in Scheme 7. In these mechanisms, the inhibitor first binds to the active site and undergoes ArO–S bond cleavage, and it is the resulting species, HSO_3NH^- or SO_2NH, that adds to the FGly carbonyl group.

CONCLUSION

Despite the superficial similarity of phosphate and sulfate esters, the stability of alkyl sulfate monoesters toward hydrolysis exceeds that of alkyl phosphate monoester dianions by 6 orders of magnitude.[27] Type I sulfatases, which hydrolyze alkyl and

dx.doi.org/10.1021/jo4026513 | J. Org. Chem. 2014, 79, 1995–2005

Scheme 7. Two Possible Mechanisms for FGly Imine *N*-Sulfate Formation

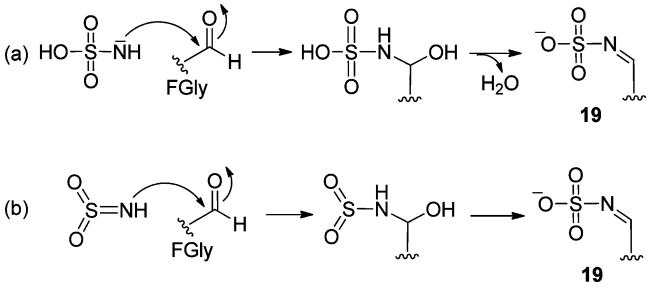

aryl sulfate monoesters through S−O bond cleavage, are the most proficient enzyme catalysts identified to date, providing rate accelerations up to 10^{26}-fold for alkyl sulfate monoester hydrolysis.[27] Quantum mechanical calculations give insight into the mechanisms of hydrolysis of aryl sulfates and sulfamates, both in solution and in the active sites of sulfatases. The uncatalyzed alkaline hydrolyses of aryl sulfates and sulfamates follow different mechanisms (S_N2 for sulfates; S_N1 for sulfamates), and theory traces this difference to the ease of sulfamate dissociation leading to sulfonylamine SO_2NH. This species is low enough in energy to exist as a distinct intermediate in the alkaline hydrolysis of aryl sulfamates, whereas SO_3 is high in energy explaining why aryl sulfates undergo hydrolysis by an S_N2 mechanism.

Brønsted analysis of the FGly-dependent sulfatase *Pa*AtsA provides evidence for a mechanism that proceeds through S_N2 substitution at sulfur in the sulfate ester, with a transition state that is less dissociative than that for uncatalyzed hydrolysis. Our data provide experimental evidence that is in close accord with previous computational investigations of uncatalyzed and enzyme-catalyzed sulfate hydrolysis, which predicted a more associative transition state for the latter.[30,40] Calculations on small models of sulfatases indicate that product release from the putative FGly-sulfate intermediate displays a very large intrinsic preference to follow an E2 rather than an S_N2 pathway. The computed barriers are consistent with studies on mutants lacking the capacity for E2 elimination and also provide insight into the reason why sulfatases require the unique post-translationally installed FGly residue whereas the structurally related enzyme alkaline phosphatase utilizes a serine residue in the hydrolysis of phosphates. Finally, a range of proposed end-products of sulfatase inactivation by aryl sulfamate inhibitors have been theoretically evaluated. An inactivation mechanism comprising binding of the inhibitor at the active site followed by ArO−S bond cleavage[43] and formation of FGly imine *N*-sulfate **19** is proposed to lead to irreversible chemical transformation of the critical catalytic residue. Reversible sulfamoylation of active-site lysine and histidine residues is invoked to explain why the inactivation consumes 3−6 molecules of inhibitor per molecule of enzyme.[5] It is hoped that the theoretical insights reported here may guide future experimental efforts to detect the as-yet elusive end-product of sulfatase inactivation by aryl sulfamates.

EXPERIMENTAL SECTION

Theoretical Calculations. Quantum mechanical calculations were performed using Gaussian 09.[44] Geometry optimizations were conducted in implicit water or diethyl ether at the B3LYP/6-31+G(d) level of theory[45] with a CPCM[46] treatment of the solvent (UFF radii). Calculations on uncatalyzed hydrolyses employed optimizations in implicit water, and calculations on model enzyme-bound species employed diethyl ether to serve as an approximate model for the interior of a protein.[47] Stationary points were verified by vibrational frequency analysis, and transition states were further verified by IRC calculations.[48] Single-point energy calculations were carried out at the SCS-MP2/6-311+G(d,p) level[49] on the B3LYP-optimized geometries. Free energies in solution (1 mol/L, 25 °C) were obtained by adding the B3LYP zero-point energy, thermal corrections, and solvation energy to the SCS-MP2 gas-phase energies. We also examined the performance of several other computational methods for predicting the mechanisms of hydrolysis of sulfate and sulfamate esters, including B3LYP/aug-cc-pVTZ and B3LYP-D3/aug-cc-pVTZ. Each of these methods mirrored the SCS-MP2 data in regard to predicting the switch in mechanism from S_N2 to S_N1 on going from aryl sulfate to sulfamate; details are provided in the Supporting Information. For literature reports discussing computational issues involved in modeling hydrolyses of sulfur esters, see refs 30 and 50.

Enzyme Kinetics. Aryl sulfates used for enzyme kinetics were known compounds and were prepared by literature procedures.[32,25a] *P. aeruginosa* arylsulfatase A (*Pa*AtsA) was recombinantly expressed in *E. coli* and purified as reported previously.[5a] Kinetic measurements were performed by monitoring changes in absorbance using a UV−vis spectrophotometer at 37 °C in methacrylate cuvettes with a path length of 1 cm. The buffer was composed of 25 mM bis-tris propane and 25 mM glycine, pH 9, supplemented with 0.05% (w/v) bovine serum albumin. Extinction coefficients for the phenols and phenyl sulfates were obtained by measuring absorbances of freshly prepared stock solutions of each compound in bis-tris propane/glycine buffer, pH 9.0, at 37 °C. Detection wavelengths at maximum absorbance for each compound were obtained from literature values.[51] Rates were determined at 7−10 substrate concentrations typically spanning $K_M/3$ to $5 \times K_M$. Rates of substrate hydrolysis in the absence of enzyme over the time course of measurement (1−3 min) were insignificant. Nonlinear regression analysis of measured rates afforded values for K_M and V_{max}. The molar extinction coefficient differences ($\Delta\epsilon$ $M^{-1}cm^{-1}$) at the measured wavelength are as follows: 4-nitrophenyl, 17800 (400 nm); 4-acetamidophenyl, 1680 (288 nm); 3-chlorophenyl, 1550 (282 nm); 3-nitrophenyl, 1230 (380 nm); 4-methoxyphenyl, 1170 (296 nm); 4-chlorophenyl, 1130 (278 nm); phenyl, 920 (277 nm).

ASSOCIATED CONTENT

Supporting Information

Comparison of reaction free energy profiles, computed geometries and energies, and experimental data. This material is available free of charge via the Internet at http://pubs.acs.org.

AUTHOR INFORMATION

Corresponding Authors

*E-mail: sjwill@unimelb.edu.au.
*E-mail: e.krenske@uq.edu.au.

Notes

The authors declare no competing financial interest.

ACKNOWLEDGMENTS

We thank the Australian Research Council and the ARC Centre of Excellence for Free Radical Chemistry and Biotechnology and the Selby Foundation for financial support. High-performance computer resources were provided by the National Computational Infrastructure National Facility (Australia), the University of Queensland Research Computing Centre, and the University of Melbourne. E.D. was supported by a Sir John and Lady Higgins Scholarship. S.J.W. and E.H.K. are Future Fellows funded by the Australian Research Council.

REFERENCES

(1) Hagelueken, G.; Adams, T. M.; Wiehlmann, L.; Widow, U.; Kolmar, H.; Tümmler, B.; Heinz, D. W.; Schubert, W.-D. *Proc. Natl. Acad. Sci. U.S.A.* **2006**, *103*, 7631−7636.

(2) Schmidt, B.; Selmer, T.; Ingendoh, A.; von Figura, K. *Cell* **1995**, *82*, 271−278.

(3) For leading reviews, see: (a) Hanson, S. R.; Best, M. D.; Wong, C.-H. *Angew. Chem., Int. Ed.* **2004**, *43*, 5736−5763. (b) Bojarová, P.; Williams, S. J. *Curr. Opin. Chem. Biol.* **2008**, *12*, 573−581.

(4) (a) Purohit, A.; Williams, G. J.; Howarth, N. M.; Potter, B. V. L; Reed, M. J. *Biochemistry* **1995**, *34*, 11508−11514. (b) Woo, L. W. L.; Purohit, A.; Reed, M. J.; Potter, B. V. L. *J. Med. Chem.* **1996**, *39*, 1349−1351. (c) Woo, L. W. L.; Howarth, N. M.; Purohit, A.; Hejaz, H. A. M.; Reed, M. J.; Potter, B. V. L. *J. Med. Chem.* **1998**, *41*, 1068−1083. (d) Woo, L. W. L.; Purohit, A.; Malini, B.; Reed, M. J.; Potter, B. V. L. *Chem. Biol.* **2000**, *7*, 773−791. (e) Hanson, S. R.; Whalen, L. J.; Wong, C.-H. *Bioorg. Med. Chem.* **2006**, *14*, 8386−8395. (f) Woo, L. W. L.; Leblond, B.; Purohit, A.; Potter, B. V. L. *Bioorg. Med. Chem.* **2012**, *20*, 2506−2519.

(5) (a) Bojarová, P.; Denehy, E.; Walker, I.; Loft, K.; De Souza, D. P.; Woo, L. W. L.; Potter, B. V. L.; McConville, M. J.; Williams, S. J. *ChemBioChem* **2008**, *9*, 613−623. (b) For studies on a range of other sulfatases, see: Bojarová, P.; Williams, S. J. *Bioorg. Med. Chem. Lett.* **2009**, *19*, 477−480.

(6) (a) Williams, S. J. *Exp. Opin. Ther. Pat.* **2013**, *23*, 79−98. (b) Stanway, S. J.; Purohit, A.; Woo, L. W. L.; Sufi, S.; Vigushin, D.; Ward, R.; Wilson, R. H.; Stanczyk, F. Z.; Dobbs, N.; Kulinskaya, E.; Elliott, M.; Potter, B. V. L.; Reed, M. J.; Coombes, R. C. *Clin. Cancer Res.* **2006**, *12*, 1585−1592. (c) Stanway, S. J.; Delavault, P.; Purohit, A.; Woo, L. W. L.; Thurieau, C.; Potter, B. V. L.; Reed, M. J. *Oncologist* **2007**, *12*, 370−374. (d) Woo, L. W. L.; Purohit, A.; Potter, B. V. L. *Mol. Cell. Endocrinol.* **2011**, *340*, 175−185.

(7) Ghosh, D. *Methods Enzymol.* **2005**, *400*, 273−293.

(8) Bond, C. S.; Clements, P. R.; Ashby, S. J.; Collyer, C. A.; Harrop, S. J.; Hopwood, J. J.; Guss, J. M. *Structure* **1997**, *5*, 277−289.

(9) Lukatela, G.; Krauss, N.; Theis, K.; Selmer, T.; Gieselmann, V.; von Figura, K.; Saenger, W. *Biochemistry* **1998**, *37*, 3654−3664.

(10) Recksiek, M.; Selmer, T.; Dierks, T.; Schmidt, B.; von Figura, K. *J. Biol. Chem.* **1998**, *273*, 6096−6103.

(11) Hollfelder and co-workers reported (ref 14b) that the C51S and C51A mutants of *Pa*AtsA exhibit reductions in k_{cat}/K_M by 2330- and 327000-fold, respectively, and that the former mutant enzyme is capable of turnover. These reductions in k_{cat}/K_M are on the order of, or greater than, the estimated rates of translational misincorporation (10^{-3} to 10^{-4}). (Kramer, E. B.; Farabaugh, P. J. *RNA* **2007**, *13*, 87−96). Furthermore, the similarity of K_M values observed for the mutants and wildtype enzymes suggests that the observed turnover of these species arises not from the intrinsic low activity of the mutant enzyme but rather from contaminating wildtype enzyme. (Schimmel, P. *Acc. Chem. Res.* **1989**, *22*, 232−233). von Figura and co-workers reached a similar conclusion when studying the C69S mutant of human arylsulfatase A (ref 10).

(12) Brooks, D. A.; Robertson, D. A.; Bindloss, C.; Litjens, T.; Anson, D. S.; Peters, C.; Morris, C. P.; Hopwood, J. J. *Biochem. J.* **1995**, *307*, 457−463.

(13) Cleland, W. W.; Hengge, A. C. *Chem. Rev.* **2006**, *106*, 3252−3278.

(14) (a) Babtie, A. C.; Bandyopadhyay, S.; Olguin, L. F.; Hollfelder, F. *Angew. Chem., Int. Ed.* **2009**, *48*, 3692−3694. (b) Olguin, L. F.; Askew, S. E.; O'Donoghue, A. C.; Hollfelder, F. *J. Am. Chem. Soc.* **2008**, *130*, 16547−16555.

(15) Jonas, S.; van Loo, B.; Hyvönen, M.; Hollfelder, F. *J. Mol. Biol.* **2008**, *384*, 120−136.

(16) Benkovic, S. J.; Benkovic, P. A. *J. Am. Chem. Soc.* **1966**, *88*, 5504−5511.

(17) Fendler, E. J.; Fendler, J. H. *J. Org. Chem.* **1968**, *33*, 3852−3859.

(18) Hoff, R. H.; Larsen, P.; Hengge, A. C. *J. Am. Chem. Soc.* **2001**, *123*, 9338−9344.

(19) Lowe et al. reported an isotopic labeling study that ruled out the intermediacy of free SO_3 in the alcoholysis of tetrabutylammonium phenylsulfate in CCl_4. See: Chai, C. L. L.; Hepburn, T. W.; Lowe, G. *J. Chem. Soc., Chem. Commun.* **1991**, 1403−1405.

(20) Hopkins, A.; Day, R. A.; Williams, A. *J. Am. Chem. Soc.* **1983**, *105*, 6062−6070.

(21) Thea, S.; Cevasco, G.; Guanti, G.; Williams, A. *J. Chem. Soc., Chem. Commun.* **1986**, 1582−1583.

(22) Douglas, K. T.; Williams, A. *J. Chem. Soc., Chem. Commun.* **1973**, 356.

(23) (a) Spillane, W. J.; Hogan, G.; McGrath, P. *J. Phys. Org. Chem.* **1995**, *8*, 610−616. (b) McCaw, C. J. A.; Spillane, W. J. *J. Phys. Org. Chem.* **2006**, *19*, 512−517. (c) Spillane, W. J.; McCaw, C. J. A.; Maguire, N. P. *Tetrahedron Lett.* **2008**, *49*, 1049−1052. (d) Spillane, W. J.; Malaubier, J.-B. *Tetrahedron Lett.* **2010**, *51*, 2059−2062. (e) Spillane, W. J.; Thea, S.; Cevasco, G.; Hynes, M. J.; McCaw, C. J. A.; Maguire, N. P. *Org. Biomol. Chem.* **2011**, *9*, 523−530.

(24) Williams, A.; Douglas, K. T. *J. Chem. Soc., Perkin Trans. 2* **1974**, 1727−1732.

(25) For crystallographic and theoretical studies of aryl sulfate and sulfamate structure−reactivity trends, see: (a) Denehy, E.; White, J. M.; Williams, S. J. *Chem. Commun.* **2006**, 314−316. (b) Denehy, E.; White, J. M.; Williams, S. J. *Inorg. Chem.* **2007**, *46*, 8871−8886.

(26) Burlingham, B. T.; Pratt, L. M.; Davidson, E. R.; Shiner, V. J., Jr.; Fong, J.; Widlanski, T. S. *J. Am. Chem. Soc.* **2003**, *125*, 13036−13037.

(27) Edwards, D. R.; Lohman, D. C.; Wolfenden, R. *J. Am. Chem. Soc.* **2012**, *134*, 525−531.

(28) The earlier study of Fendler and Fendler (ref 17) reported a β_{LG} value of −1.2 for hydrolysis at 100 °C.

(29) For leading reviews, see: (a) Bentzien, J.; Florián, J.; Glennon, T. M.; Warshel, A. In *Combined Quantum Mechanical and Molecular Mechanical Methods*; Gao, J., Thompson, M. A., Eds.; ACS Symposium Series 712; American Chemical Society: Washington, DC, 1998; pp 16−34. (b) Nam, K.; Gao, J.; York, D. M. In *Multiscale Simulation Methods for Nanomaterials*; Ross, R. B., Mohanty, S., Eds.; John Wiley & Sons, Inc.: Hoboken, NJ, 2007; Chapter 12. (c) Kamerlin, S. C. L.; Haranczyk, M.; Warshel, A. *ChemPhysChem* **2009**, *10*, 1125−1134. (d) Kamerlin, S. C. L.; Sharma, P. K.; Prasad, R. B.; Warshel, A. *Q. Rev. Biophys.* **2013**, *46*, 1−132.

(30) Kamerlin, S. C. L. *J. Org. Chem.* **2011**, *76*, 9228−9238.

(31) The potential energy surfaces for cleavage of the PhO−S bonds of **3** and **4** (and formation of the HO−S bond of the products) were explored by performing constrained optimizations in which the relevant O−S bond of PhO−SO_2X^- or HO−SO_2X^- (X = O, NH) was stretched incrementally. The potential energy was found to increase smoothly for stretching up to at least 1.7 Å. In the case of the dissociation of **4**, the corresponding free energy surface was also computed and was likewise found to contain no maximum when stretching the PhO−S bond up to 1.7 Å.

(32) Experimental rate constants for alkaline hydrolysis of **1** and **2** have been reported. For **1**, Hengge et al. (ref 18) report the following values at pH 9.0 and 35 °C: $\Delta H^{\ddagger}$ = 24.4 kcal/mol, $\Delta S^{\ddagger}$ = −19.5 eu, $\Delta G^{\ddagger}$ = 30.4 kcal/mol. For **2**, the data of Thea et al. (ref 21) provide a rate constant at pH 9.0 and 25 °C of $k = 1.1 \times 10^{-1}$ s^{-1}, from which $\Delta G^{\ddagger}$ = 19 kcal/mol. The theoretical calculations are in qualitative agreement with the experimental $\Delta G^{\ddagger}$ values, insofar as they predict that sulfamate **2** reacts faster than sulfate **1**. More detailed quantitative comparisons with the experimental activation parameters are not possible, however, because the calculations only consider those processes that occur after deprotonation of **1** or **2**, rather than the full reaction pathway, and are subject to errors associated with the use of OH^- as nucleophile and with the calculation of entropies in solution.

(33) (a) Truce, W. E.; Campbell, R. W.; Norell, J. R. *J. Am. Chem. Soc.* **1964**, *86*, 288. (b) Opitz, G. *Angew. Chem., Int. Ed.* **1967**, *6*, 107−123. (c) King, J. F. *Acc. Chem. Res.* **1975**, *8*, 10−17. (d) King, J. F.; Lam, J. Y. L.; Skonieczny, S. *J. Am. Chem. Soc.* **1992**, *114*, 1743−1749. (e) Lyashchuk, S. N.; Skrypnik, Y. G.; Besrodnyi, V. P. *J. Chem. Soc., Perkin Trans. 2* **1993**, 1153−1159.

(34) (a) Davy, M. B.; Douglas, K. T.; Loran, J. S.; Steltner, A.; Williams, A. *J. Am. Chem. Soc.* **1977**, *99*, 1196−1206. (b) Vizgert, R. V.; Kachanko, I. E. *Reakts. Sposobn. Org. Soedin.* **1968**, *5*, 9−26 (CA 69:76105).
(35) (a) Dodgson, K. S.; Spencer, B.; Williams, K. *Biochem. J.* **1956**, *64*, 216−221. (b) Benkovic, S. J.; Vergara, E. V.; Hevey, R. C. *J. Biol. Chem.* **1971**, *246*, 4926−4933.
(36) Boltes, I.; Czapinska, H.; Kahnert, A.; von Bulow, R.; Dierks, T.; Schmidt, B.; von Figura, K.; Kertesz, M. A.; Uson, I. *Structure* **2001**, *9*, 483−491.
(37) Values of $\Delta\Delta G^{\ddagger}$ and $\Delta\Delta H^{\ddagger}$ are calculated with respect to the isolated reactants (**3** + imidazole + water + $MeCR(OH)O^{-}$ (R = H or OH)).
(38) Marino, T.; Russo, N.; Toscano, M. *Chem.—Eur. J.* **2013**, *19*, 2185−2192.
(39) Chruszcz, M.; Laidler, P.; Monkiewicz, M.; Ortlund, E.; Lebioda, L.; Lewinski, K. *J. Inorg. Biochem.* **2003**, *96*, 386−392.
(40) Kamerlin and co-workers recently reported EVB studies of *Pa*AtsA-catalyzed sulfate and phosphate ester hydrolysis. Their studies examined the sulfate/phosphate transfer step and gave detailed consideration to the roles of acidic and basic residues. See: (a) Luo, J.; van Loo, B.; Kamerlin, S. C. L. *FEBS Lett.* **2012**, *586*, 1622−1630. (b) Luo, J.; van Loo, B.; Kamerlin, S. C. L. *Proteins* **2012**, *80*, 1211−1226.
(41) Jonas, S.; van Loo, B.; Hyvönen, M.; Hollfelder, F. *J. Mol. Biol.* **2008**, *384*, 120−136.
(42) Ahmed, S.; James, K.; Owen, C. P.; Patel, C. K.; Sampson, L. *Bioorg. Med. Chem. Lett.* **2002**, *12*, 1279−1282.
(43) *Pa*AtsA has been calculated to accelerate the cleavage of the ArO−S bond of simple aryl sulfamates by a factor of 10^4. See: Edwards, D. R.; Wolfenden, R. *J. Org. Chem.* **2012**, *77*, 4450−4453.
(44) Frisch, M. J.; Trucks, G. W.; Schlegel, H. B.; Scuseria, G. E.; Robb, M. A.; Cheeseman, J. R.; Scalmani, G.; Barone, V.; Mennucci, B.; Petersson, G. A.; Nakatsuji, H.; Caricato, M.; Li, X.; Hratchian, H. P.; Izmaylov, A. F.; Bloino, J.; Zheng, G.; Sonnenberg, J. L.; Hada, M.; Ehara, M.; Toyota, K.; Fukuda, R.; Hasegawa, J.; Ishida, M.; Nakajima, T.; Honda, Y.; Kitao, O.; Nakai, H.; Vreven, T.; Montgomery, J. A., Jr.; Peralta, J. E.; Ogliaro, F.; Bearpark, M.; Heyd, J. J.; Brothers, E.; Kudin, K. N.; Staroverov, V. N.; Kobayashi, R.; Normand, J.; Raghavachari, K.; Rendell, A.; Burant, J. C.; Iyengar, S. S.; Tomasi, J.; Cossi, M.; Rega, N.; Millam, N. J.; Klene, M.; Knox, J. E.; Cross, J. B.; Bakken, V.; Adamo, C.; Jaramillo, J.; Gomperts, R.; Stratmann, R. E.; Yazyev, O.; Austin, A. J.; Cammi, R.; Pomelli, C.; Ochterski, J. W.; Martin, R. L.; Morokuma, K.; Zakrzewski, V. G.; Voth, G. A.; Salvador, P.; Dannenberg, J. J.; Dapprich, S.; Daniels, A. D.; Farkas, Ö.; Foresman, J. B.; Ortiz, J. V.; Cioslowski, J.; Fox, D. J. Gaussian 09, Revision C.01, Gaussian, Inc., Wallingford, CT, 2009.
(45) (a) Lee, C.; Yang, W.; Parr, R. G. *Phys. Rev. B* **1988**, *37*, 785−789. (b) Becke, A. D. *J. Chem. Phys.* **1993**, *98*, 1372−1377. (c) Becke, A. D. *J. Chem. Phys.* **1993**, *98*, 5648−5652. (d) Stephens, P. J.; Devlin, F. J.; Chabalowski, C. F.; Frisch, M. J. *J. Phys. Chem.* **1994**, *98*, 11623−11627.
(46) (a) Barone, V.; Cossi, M. *J. Phys. Chem. A* **1998**, *102*, 1995−2001. (b) Cossi, M.; Rega, N.; Scalmani, G.; Barone, V. *J. Comput. Chem.* **2003**, *24*, 669−681.
(47) Zhang, X.; DeChancie, J.; Gunaydin, H.; Chowdry, A. B.; Clemente, F. R.; Smith, A. J. T.; Handel, T. M.; Houk, K. N. *J. Org. Chem.* **2008**, *73*, 889−899.
(48) (a) Gonzalez, C.; Schlegel, H. B. *J. Chem. Phys.* **1989**, *90*, 2154−2161. (b) Gonzalez, C.; Schlegel, H. B. *J. Phys. Chem.* **1990**, *94*, 5523−5527.
(49) (a) Grimme, S. *J. Chem. Phys.* **2003**, *118*, 9095−9102. (b) Gerenkamp, M.; Grimme, S. *Chem. Phys. Lett.* **2004**, *392*, 229−235. (c) Grimme, S. *J. Phys. Chem. A* **2005**, *109*, 3067−3077.
(50) Duarte, F.; Geng, T.; Marloie, G.; Al Hussain, A. O.; Williams, N. H.; Kamerlin, S. C. L. *J. Org. Chem.* **2013**, DOI: 10.1021/jo402420t.
(51) Kempton, J. B.; Withers, S. G. *Biochemistry* **1992**, *31*, 9961−9969.